RESSALVA

Atendendo solicitação do autor,
o texto completo desta tese será
disponibilizado somente a partir
de 30/08/2020

UNIVERSIDADE ESTADUAL PAULISTA
"JÚLIO DE MESQUITA FILHO"
Câmpus de São José do Rio Preto

Airton Germano Bispo Junior

Light-emitting diodes based on Eu^{3+}, Eu^{2+} or Tb^{3+}-doped silicates for lighting and Circadian rhythm regulation

São José do Rio Preto
2019

Airton Germano Bispo Junior

Light-emitting diodes based on Eu^{3+}, Eu^{2+} or Tb^{3+}-doped silicates for lighting and Circadian rhythm regulation

Tese apresentada como parte dos requisitos para obtenção do título de Doutor em química, junto ao Programa de Pós-Graduação em Química, do Instituto de Biociências, Letras e Ciências Exatas da Universidade Estadual Paulista "Júlio de Mesquita Filho", Câmpus de São José do Rio Preto.

Financiadora: FAPESP – Proc.. 2016/20421-9

CAPES

Orientadora: Profª. Drª. Ana Maria Pires

Coorientador: Prof. Dr. Sergio Antonio Marques de Lima

São José do Rio Preto

2019

B622l

Bispo Junior, Airton Germano

Light-emitting diodes based on Eu3+, Eu2+ or Tb3+-doped silicates for lighting and circadian rhythm regulation / Airton Germano Bispo Junior. -- São José do Rio Preto, 2019

178 f. : il., tabs.

Tese (doutorado) - Universidade Estadual Paulista (Unesp), Instituto de Biociências Letras e Ciências Exatas, São José do Rio Preto

Orientadora: Ana Maria Pires

Coorientador: Sergio Antonio Marques Lima

1. LEDs. 2. Iluminação de estado sólido. 3. Terras raras. 4. Sol-gel. 5. Luminescência. I. Título.

Sistema de geração automática de fichas catalográficas da Unesp. Biblioteca do Instituto de Biociências Letras e Ciências Exatas, São José do Rio Preto. Dados fornecidos pelo autor(a).

Essa ficha não pode ser modificada.

Airton Germano Bispo Junior

Light-emitting diodes based on Eu^{3+}, Eu^{2+} or Tb^{3+}-doped silicates for lighting and Circadian rhythm regulation

Tese apresentada como parte dos requisitos para obtenção do título de Doutor em química, junto ao Programa de Pós-Graduação em Química, do Instituto de Biociências, Letras e Ciências Exatas da Universidade Estadual Paulista "Júlio de Mesquita Filho", Câmpus de São José do Rio Preto.

Financiadora: FAPESP – Proc.. 2016/20421-9

CAPES

Comissão Examinadora

Profª. Drª. Ana Maria Pires
UNESP – Campus de Presidente Prudente
Orientadora

Profª. Drª. Marian Rosaly Davolos
UNESP – Campus de Araraquara

Prof. Dr. Fernando Aparecido Sigoli
UNICAMP

Prof. Dr. Carlos José Leopoldo Constantino
UNESP - Campus de Presidente Prudente

Prof. Dr. Paulo Cesar de Sousa Filho
UNICAMP

Presidente Prudente
30 de agosto de 2019

To my parents Maria José Santander Bispo and Airton Germano Bispo

ACKNOWLEDGEMENTS

My parents Maria José Santander Bispo and Airton Germano Bispo for sure are the real responsible for this study because they always encouraged me to study and highlighted me how education can change someone's life. Fortunately, I got the opportunity to be born into a family with the opportunity of enabling my education and I am very proud of that. For giving me the inspiration to be a good person. Everything is for you!

I thank my sister Michele Santander Bispo and my niece Julia Maria Bispo Reis for the companionship. It is worth pointing out the importance of my aunts Maria Antonia Santander dos Anjos, Ivone Santander Tardim, Nair Santander, my uncle Roberto Santander and my cousins Carla Santander dos Anjos, Carlos Romão Santander dos Anjos Souza and Andrea Santander dos Anjos in my life and in my education. My grandfather Romão Santander (*in memoriam*) and grandmother Alice Santander Centeio (*in memoriam*) for being with me all the time, taking care of me.

Professor Ana M. Pires opened the doors of her lab and introduced me to the luminescence subject, something that now I am fascinated with. She is also an inspiration of the kind of person and professional I want to be: smart, hardworking, kind, polite, and ethical. Professor Sergio A. M. de Lima, co-head of LLuMes group, is acknowledged for my scientific education during the graduation and Ph.D., for the help in writing papers, data interpretation, and discussion. I also thank both for their friendship.

All my university classmates: Fernanda, Monica, Jéssica, Ariane and André for sharing with me hard study moments and friendship. A memorable acknowledge to my buddy André for all the friendship and help, my housemate Edy for the friendship, and Nagyla and Rebeca for sharing happy moments with me. All my friends of LLuMes for the companionship and the scientific discussions: André, Alessandra, Alessandro, Bianca, Bruno, Camila, Edy, Felipe, Filipe, João, Leonardo, Luis, Nagyla, Rebeca, Renan, Rodolpho and Vytor.

Professors Luis D. Carlos and Rute A. S. Ferreira for opening the doors of their lab in Aveiro and giving me the opportunity to finish my study. A special thanks to Professor Rute Ferreira for all the patience in teaching me some fundamentals on rare-earth spectroscopy and helping me in writing papers, data interpretation, and discussion. All my fellows from Aveiro: Caixeta, Fernanda, Fernando, Gosia, Joana Costa, João

Ramalho, Justyna, Rita Bastos, Rita Frias, Luis, Rodolfo, Sofia, and Talita for making easier my stay in Portugal.

All the collaborators of this study:

Professor Celso X. Cardoso for the synthesis with PVDF and BO.

LAB-MEV and MSc Glenda G. Souza for MEV measurements.

Sol-gel research group from UNIFRAN coordinated by Professors Eduardo J. Nassar and Professor Lucas A. Rocha for the photoluminescence measurements.

Laboratório Multiusuário de análises químicas of IQ-UNESP and Alberto C. Alécio and Naira C. Pesquero for the diffuse reflectance measurements.

Laboratório de difração de raios X coordinated by Professor Silvio R. Teixeira and MSc Wagner D. Macedo Júnior for the XRD measurements.

Núcleo de inovação tecnológica em borracha natural coordinated by Professor Aldo E. Job for the thermal analysis measurements.

Laboratório de compósitos e cerâmica funcional coordinated by Professor Silvania Lanfredi Nobre and MSc Fabiano R. Prachedes, Leonardo P. de M. Simões, MSc Gisele S. Silveira and MSc Eliane A. Namikuchi for the XRD measurements.

Laboratório de filmes nanoestruturados e espectroscopia coordinated by Professor Carlos J. L. Constantino, and Dr. Sabrina A. Camacho, MSc José D. Fernandes, MSc Rafael J. G. Rubira and Dr. Cibely da S. Martin for Raman measurements.

University of Aveiro, Professors Luís D. Carlos and Rute A. S. Ferreira for receiving me in phantom-g.

Dr. Carlos D. S. Brites from phantom-g for the quantum yield measurements.

Dr. Alexandre M. P. Botas and Dr. Sandra F. H. Correia from phantom-g for helping me with the photoluminescence measurements.

MSc Marita A. Cardoso for the help with the fabrication of PMMA films.

Dr. Andrei Kovalevsky from CICECO for the help in the heat treatments.

Dr. Rosário T. Soares from Chemistry department of University of Aveiro for XRD measurements and Rietveld Refinement.

I thank IBILCE and the post-graduation in chemistry.

This work was carried out with the support of the Coordination of Superior Level Staff Improvement - Brazil (CAPES) - Financing Code 001, to which I thank.

I thank FAPESP for granting the research grant under process no. 2016/20421-9 São Paulo Research Foundation - FAPESP (FAPESP).

“[…] Hey you, don't tell me there's no hope at all,

Together we stand, divided we fall”

Gilmour, D.; Manson, N.; Waters, R.; Wright, R.
The wall, Harvest Records, 4 vinyl, track 1 (Vinyl 2).

RESUMO

Diodos emissores de luz branca (WLEDs) são as principais fontes de luz branca para iluminação e fundo de tela de displays devido ao alto brilho (800 lm) e eficácia luminosa (150 $lm \cdot W^{-1}$), alto tempo de vida útil (50.000 horas), baixo consumo energético (8,5 W), baixo preço (60 dólares em 20 anos de uso) e baixa toxicidade comparados a lâmpadas incandescentes e fluorescentes. Além dos WLEDs, LEDs monocromáticos têm ganhado atenção nos últimos anos devido ao comum consenso e entendimento da influência da luz na regulação do ritmo circadiano Humano e de plantas. Entretanto, os principais desafios são obter WLEDs com parâmetros ópticos de temperatura de cor correlata (4.500 K) e índice de renderização de cor (> 90) desejáveis e contornar o "*green gap*" na fabricação de LEDs emissores de luz verde. Desta forma, o objetivo desta tese de doutorado foi fabricar LEDs emissores de luz branca ou monocromática para iluminação, luz de tráfico e controle do ritmo circadiano. Para esta proposta, luminóforos emissores de luz verde ($Ba_2SiO_4:Eu^{2+}$ e $Ba_2SiO_4:Tb^{3+}$), amarela ($Sr_2SiO_4:Eu^{2+}$) e vermelha ($Ba_2SiO_4:Eu^{3+}$) foram sintetizados pela metodologia sol-gel, caracterizados e dispersos em filmes poliméricos (PVDF ou PMMA), aos quais foram utilizados para recobrir LEDs emissores na região espectral do UV. As condições de síntese dos luminóforos foram variadas a fim de otimizar a composição das fases e a emissão dos dopantes. A dispersão dos luminóforos em PMMA potencializa a emissão dos ativadores luminescentes, sendo que os luminóforos baseados em $Ba_2SiO_4:Eu^{3+}$ e $Ba_2SiO_4:Tb^{3+}$ mostram potencial para serem combinados a LEDs UV (250 nm), fazendo um dispositivo multifuncional que emite luz e também radiação UV, importante para o controle do ritmo circadiano de plantas e desinfecção em agricultura (cultivo *indoor*). Já os LEDs emissores de luz verde construídos combinando LEDs UV (365 nm) e filmes de $Ba_2SiO_4:Eu^{2+}$/PMMA apresentaram eficácia luminosa e estabilidade radiante entre as melhores reportadas, sendo uma alternativa para suprir a ausência de LEDs emissores de luz verde com alta eficácia luminosa. Finalmente, WLEDs construídos combinando LEDs UV (395 nm) e filmes de $Sr_2SiO_4:Eu^{2+}$/BAM:Eu^{2+}/PMMA apresentaram valores de eficácia luminosa e estabilidade radiante entre os melhores reportados e temperatura de cor dependente da proporção dos luminóforos, podendo ser ajustada para aplicações em iluminação diurna (CCT = 6.000 K) e noturna (CCT = 4.500 K), além de usos em fototerapia.

Palavras-chaves: LEDs. Iluminação de estado sólido. Terras raras. Sol-gel. Luminescência.

ABSTRACT

White-light-emitting diodes (WLEDs) are the main light sources for indoor and outdoor lightings as well as for backlighting of displays due to their high brightness (800 lm) and luminous efficacy (150 $lm \cdot W^{-1}$), long lifespan (50,000 hours), low power consumption (8.5 W), low cost (60 dollars over 20 years of use) and environmentally friendly properties compared to the traditional incandescent and fluorescent bulbs. Beyond WLEDs, attention has currently been paid to monochromatic LEDs due to the common consensus on the light impact on human and plant circadian rhythm regulation. Nonetheless, the main challenges are to come up with WLEDs featuring desirable correlated color temperature (4,500 K) and color rendering index (> 90) and work around the "green gap" drawback in the fabrication of green-emitting LEDs. Therefore, the goal of this Ph.D. thesis is to report on the fabrication of white or monochromatic-emitting LEDs, and for this propose, UV-to-green ($Ba_2SiO_4:Eu^{2+}$ e $Ba_2SiO_4:Tb^{3+}$), yellow ($Sr_2SiO_4:Eu^{2+}$) and red ($Ba_2SiO_4:Eu^{3+}$) downshifting converter phosphors were synthesized by the sol-gel route, fully characterized and dispersed as polymeric films (PVDF or PMMA), to which were used to coat commercial UV LEDs. The synthesis conditions of the phosphors were changed aiming to optimize phase composition and emission intensity of the dopants. PMMA plays the role of enhancing the luminescent activator emission, and both $Ba_2SiO_4:Eu^{3+}$ and $Ba_2SiO_4:Tb^{3+}$ phosphors feature the required characteristics to be used as coatings of UV LEDs (250 nm), making multifunctional prototypes emitting UV and red light for simultaneous application in indoor farms by regulating the plant circadian rhythm and as a disinfection agent. On the other hand, the green-emitting LEDs built by coating UV LEDs (365 nm) with $Ba_2SiO_4:Eu^{2+}$/PMMA films match high luminous efficacy and radiant stability, among the best values reported so far, being a practicable alternative to supply the absence of commercially-available high-efficient green-emitting LEDs. Finally, WLED prototypes built by combining UV LEDs (395 nm) and $Sr_2SiO_4:Eu^{2+}$/BAM:Eu^{2+}/PMMA films display luminous efficacy and radiant stability among the best reported, and correlated color temperature depending on the phosphor mixture proportion, that may be tuned for daylight (6,000 K) and night light (3,500 K) applications, as well as phototherapy and backlighting of displays.

Keywords: LEDs. Solid-state lighting. Rare earth. Sol-gel. Luminescence.

LIST OF FIGURES

LIST OF TABLES

LIST OF ABBREVIATIONS

365-B LED	Green-emitting LED prototype
B2S	$Ba_2SiO_4:Eu^{2+}$
Ba_9	Barium site in Ba_2SiO_4 with CN = 9
Ba_{10}	Barium site in Ba_2SiO_4 with CN = 10
BO	Buriti oil
BSXEu	Eu-doped Ba_2SiO_4 (X %) calcinated for 2 hours
BSXEuYTb	Eu and Tb-doped Ba_2SiO_4
BSXTb	Tb-doped Ba_2SiO_4 (X %)
CD	Carbon dot
CCT	Correlated color temperature
CFL	Compact fluorescent lamp
CIE	1,931 *Commission internationale de l'éclairage*
CRI	Color rendering index
CM-LED	Color-mixed LED
CN	Coordination number
CR	Cross-relaxation
CTB1	Charge transfer band from Eu^{3+} in Ba local sites
CTB2	Charge transfer band from Eu^{3+} -O^{2-} associates
D	Donator specie
D*	Excited donator specie
D-D	Dipole-dipole
D_{ED}	Electric dipole strength
D_{MD}	Magnetic dipole strength
DSC	Differential scanning calorimetry
D-Q	Dipole-quadrupole
DR	Diffuse reflectance spectroscopy
DTG	Differential thermal analysis
DRX	X-ray diffraction
ED	Electric dipole oscillator
EDS	Energy-dispersive X-ray spectroscopy
EHT	Electron high tension
EM	Magnetic dipole oscillator
E_{photon}	Energy of a photon
EQ	Electric quadrupole oscillator
EQE	External quantum efficiency
ET	Energy transfer
Eu_{1-3}	Eu local sites in Ba_2SiO_4 or $BaSiO_3$ lattice
$Eu_{A1,2}$	Eu local sites related to Eu^{3+}-O^{2-} associates
Eu_{D1-3}	Defect-related Eu local sites
FTIR	Fourier transform infrared spectroscopy
FWHM	Full-width-at-half-maximum
HID	High-intensity discharge lamp
ICDD	International Centre for Diffraction Data
ipRGCs	Intrinsically photosensitive retinal ganglion cells
IR	Infrared radiation
LE	Luminous efficacy
LED	Light-emitting diodes

Ln-X	Ba_2SiO_4: Ln (Ln = Eu or Gd) and X = 2 h and 10 h (calcination time)
MW	Molar weight
Near-UV LED	Near-UV-emitting LED chip
OLED	Organic light-emitting diode
PC-LED	Phosphor-converted LED
PL	Photoluminescence
PLE	Excitation spectrum
PLED	Polymer light-emitting diode
PMMA	Poly(methyl methacrylate)
PMMA:MEu-X	PMMA films with different amount of BSEu
PVDF	Polyvinylidene fluoride
PVDF:XBO	PVDF films with X mL of BO
PVDF:yBSEu	PVDF films with 400 mL of BO and different amount of BS4Eu
$\boldsymbol{P_{eletric}}$	Electric power
$\boldsymbol{P_{optical}}$	Optical power
QD	Quantum dots
Q-Q	Quadrupole-quadrupole
RE	Rare Earth
RGB	Red, blue and green
S2S	$Sr_2SiO_4:Eu^{2+}$
S2S(X)BAM(Y)	PMMA films doped with X % of S2S and Y % of BAM
SAD	Seasonal Affective Disorder
SD	Starting delay
SEM	Scattering electron microscope
SI	International System of Units
SMD	Surface mounted LED
Sr_9	Strontium site in Sr_2SiO_4 with CN = 9
Sr_{10}	Strontium site in Sr_2SiO_4 with CN = 10
SSL	Solid-state lighting
$T_{calc.}$	Calcination temperature
Td	Fluorescent bulb with 15.9 mm of diameter
TEM	Transmission electron microscopy
TEOS	Tetraethyl orthosilicate
TG	Thermogravimetric analysis
TWh	Terawatt-hour
UV	UV radiation
WPE	Wall-plug efficiency
WLED	White-emitting LED
XRD	X ray diffraction
YAG	Yttrium Aluminium Garnet
ZPL	Zero-phonon line

LIST OF SYMBOLS

10Dq	Strength of the ligand field
$^{2S+1}L_J$	Russell-Saunders term
(x,y)	1,931 CIE color coordinates
$\langle f^N \psi J \vert U^{(\lambda)} \vert f^N \psi' J' \rangle^2$	Reduced matrix elements
°C	Degree Celsius
η	Quantum efficiency of an emitting state
η_{CR}	Cross-relaxation efficiency
η_{ext}	Extraction efficiency
$\eta_{PC\text{-}LED}$	LED efficiency
η_{SA}	Self-absorption efficiency
η_{stokes}	Ratio between the energy of the excitation and emission photons
η_{yield}	Phosphor quantum yield
λ	Wavelength
λ_{em}	Emission wavelength
λ_{ex}	Excitation wavelength
τ^{rad}	Radiative lifetime
χ	Lorentzian field correction
χ^2	"Chi squared"
ϕ_V	Luminous flux
μm	Micrometer
ΔE	Thermal activation energy
ΔE_1	Energy barrier for the energy transfer from the Eu_{10} to the Eu_9 site in the Ba_2SiO_4
ΔE_2	Energy barrier for the energy transfer from the Eu9 to the Eu10 site in the Ba_2SiO_4
ΔH_m	Heat of fusion
ΔS_m	Entropy variation in the melting process
Ω_2 **e** Ω_4	Judd-Ofelt intensity parameters
A_{01}	Einstein's coefficient for spontaneous emission
Å	ångström
A	amper
A	Acceptor specie
A*	Excited acceptor specie
A_{nrad}	Non-radiative decay rate
A_{tp}	Crystal field parameters
A_{rad}	Radiative decay rate
cm	Centimeter
e	Electron charge
E_a	Electron affinity of the ligand atoms
eV	Electronvolt
g	Gram
$g \cdot cm^{-3}$	Gram per centimeter
$g \cdot mol^{-1}$	Gram per mol
h	Plank's constant
Hz	Hertz
I	Electric current
J	Total angular quantum number

$J \cdot g^{-1}$	Joule per gram
$J\ g^{-1}K^{-1}$	Joule per gram Kelvin
k	Boltzmann constant
K	Kelvin
L	Total orbital angular momentum quantum number
Lm	Lumen
Ln^{3+}	Lanthanide(III)
$lm \cdot W^{-1}$	Lumen per watts
m_e	Mass of the electron
mJ·pulse	MiliJaule per pulse
mL	Milliliter
ms	Millisecond
Mol	Mol
n	Refractive index
nm	Nanometer
P	Oscillator strength
pm	Picometer
q	Emission quantum yield
R_0	Förster distance
R_{exp}	Expected R factor
R_i	Munsell code
R_c	Critical distance
R_{WP}	weighted profile R-factor
s	Second
S	Total spin quantum number
$T_{1/2}$	Temperature at which the emission intensity is half of that at 14 K
I_T/I_{300K}	Ratio between the intensities at a given temperature T and at 300 K
T8	Fluorescent bulb with 25.5 mm of diameter
T12	Fluorescent bulb with 38.1 mm of diameter
T_g	Glass transition temperature
T_m	Melting temperature
TWh	Terawatt-hour
V	Volts
W	Watts
W_{CR}	Cross-relaxation rate

TABLE OF CONTENTS

CHAPTER 1 – INTRODUCTION

1.1 State-of-the-art

Have you ever thought how would be human life without lighting? Or better, how would society evolve in the dark? Thanks to Thomas Edison that manufactured the first electric bulb based on incandescence at the end of the XIX century, we do not ask ourselves those questions.[1] The lighting evolution has not stopped with Edison's invention since, in 1926, Edmund Germer patented the modern fluorescent lamp, opening up new opportunities of lighting by using bulbs with better efficiency and color qualities compared to incandescent sources.[2]

However, the most exciting lighting technology came up in 1996 with Shuji Nakamura at Nichia labs, who invented the first efficient white-emitting LED (WLED) based on a blue-emitting LED coated by a yellow-emitting phosphor, starting the LED boom.[2] Over the past 23 years, the luminous efficacy (LE) of WLEDs have improved from 25 lm/W to almost 200 lm/W, and this huge increase is correlated with the fabrication of high-efficient blue-light-emitting diodes by Hiroshi Amano, Shuji Nakamura, and Isamu Akasaki, who were laureates with the Nobel prize of Physics in 2014.[2]

Nowadays, WLEDs are estimated to achieve at about 60 % of penetration in 2020 in various market segments as indoor (offices, homes, shops) and outdoor (streets, traffic signals) lighting, displays (backlighting for displays, digital cameras, security equipment, mobile phone, etc.), automotive lighting and medical applications.[3,4] This huge and outstanding expansion of WLED commercialization compared to the traditional incandescent and fluorescent lamps is due to their relative low cost-benefit (60 dollars over 20 years of use), high brightness (800 lm), long lifespan (50.000 hours), compact size and shape, environmentally-friendly properties, low power consumption (8.5 W) and high LE (150 $lm.W^{-1}$), as represented in Figure 1.1 and Table 1.1.[5]

Table 1.1 Comparison of typical market prices for various lighting sources. CFL = Compact fluorescent lamp.

Lighting Source	Price ($/klm)
Halogen Lamp (A19 43W; 750 lumens)	$2.5
CFL (13W; 800 lumens)	$2
Fluorescent Lamp and Ballast System (F32T8)	$4
LED Lamp (A19 12W; 800 lumens, dimmable)	$16
LED 6" Downlight (11.5W; 625 lumens)	$43
OLED Luminaire	$1,400

Source: Adapted from Bardsley *et al.*[6]

Figure 1.1 Temporal development of the luminous efficacy of different kinds of lamps.

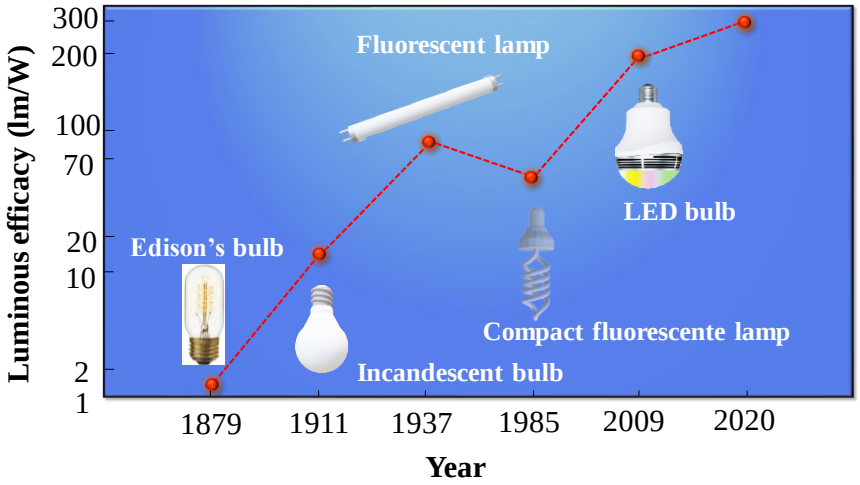

Source: Adapted from Mitch.[4]

A recent report from the US Department of energy[6] points out that the traditional bulb replacement by WLEDs is expected to reduce the lighting sector consumption by 15 % in 2020 and by 40 % in 2030, saving 261 TWh (equivalent to the total energy consumption of at about 24,000,000 homes in the US). A recent example from the commercial lighting sector is also shown in Figure 1.2, highlighting the energy saves due to the replacement of traditional bulbs by LED lamps in the US.

Figure 1.2 (a) Global commercial lighting revenue forecast, (b) Forecast of shipments of commercial lamps and luminaires. (c) Lighting inventory, electricity consumption, and lumen production. Abbreviations: HID (High-intensity discharge lamp), CFL (Compact fluorescent lamp), T12 (fluorescent bulb with 38.1 mm of diameter), T8 (fluorescent bulb with 25.5 mm of diameter), T5 (fluorescent bulb with 15.9 mm of diameter).

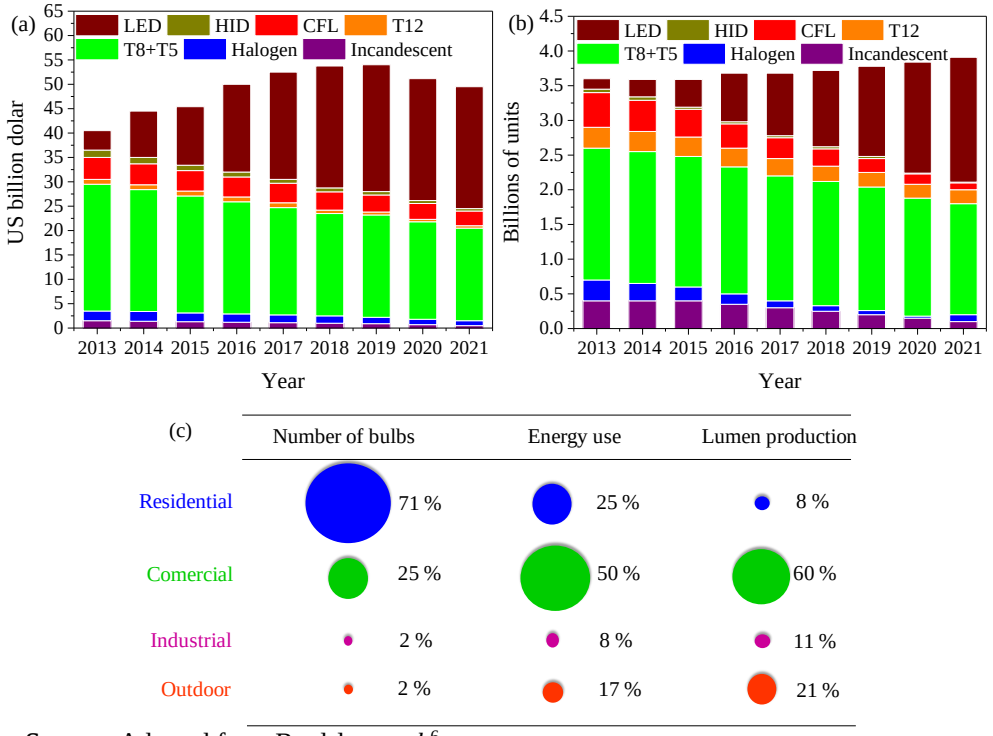

Source: Adapted from Bardsley *et al.*[6]

However, although most of the governments are providing financial support for solid-state lighting (SSL), many countries have still experienced less than 10 % of LED bulbs in the lighting market.[6] Therefore, the basic research on SSL has an enormous impact on energy savings in the world and a vast field of opportunities taking into account the improvement of WLED properties, namely the luminous efficacy and the color qualities as correlated color temperature (CCT) and color rendering index (CRI).[4]

The main commercially-available WLED is based on the combination of the GaN blue-emitting LED chip and the blue-to-yellow downshifting converter $Y_3Al_5O_{12}$: Ce^{3+} (YAG:Ce^{3+} - Yttrium Aluminium Garnet) phosphor.[7] The combination of the yellow with the remaining blue light generates a bluish-white light sensation to the human eye. Yet, although this approach displays high LE, it also features high CCT dependent on the operating voltage and time of use, and poor CRI due to the absence of red-emitting components.[8] It is important to point out that much attention has currently been paid to the color qualities of WLEDs since, in the last few years, many studies have shown that light has a huge impact on the human circadian rhythm.[9] Those disadvantages, combined to the higher price compared to the traditional lighting bulbs, create a barrier between the customer and the WLED market, even that its lifespan is immensely higher.[5]

In order to overcome those issues, the SSL engineering is now focused on three different research fields: (1) the fabrication of high-efficient and stable blue-to-red downshifting-converter phosphors to improve the CRI and decrease the CCT of the YAG-based WLED, (2) the fabrication of high-efficient near-UV-to-visible downshifting converter phosphors to be used as coatings of near-UV-emitting LEDs because the human eye does not see UV radiation, solving the CCT stability problem or (3) the fabrication of high-efficient and stable green or red-emitting semiconductor LED chips to be combined to the blue-emitting chip.[6]

However, for the best of our knowledge, all the compositions with red-emitting phosphors for the issue (1) decrease the luminous efficacy of the YAG-based LED, as shown in the figure of merit of LE, CCT and CRI, Table 1.2. Furthermore, the human eye does not have good sensitivity in the red spectral region, requiring high amounts of red-emitting phosphor in the LED composition to be detected by the retina.[10] For issue (2), there is a lack of high-efficient and stable near-UV-to-visible downshifting converter phosphors. Considering issue (3), there is a lack of green-emitting semiconductor materials that is known as “green-gap”, minutely discussed as follow.[11]

Table 1.2 State-of-the-art of WLEDs comparing luminous efficacy (LE), correlated color temperature (CCT) and color rendering index (CRI) as figures of merit. The values reported for incandescent and fluorescent lamps are also reported.

Composition	LED chip / nm	LE / $lm.W^{-1}$	CCT / K	CRI	[ref]
Incandescent [1]	-	26	2,812	43	12
Fluorescent [2]	-	60	3,753	100	12
YAG	460	164	5,468	78	12
YAG and $K_2GeF_6:Mn^{4+}$	460	125	3,882	90.4	13
YAG and $K_2SiF_6:Mn^{4+}$	460	116	3,900	89.9	14
YAG and $K_2(Si,Ge)F_6:Mn^{4+}$	460	145.33	6,110	70.5	15
YAG and $CsNaGeF_6:Mn^{4+}$	460	176.3	3,783	92.5	16
YAG and $Rb_3AlF_6:Mn^{4+}$	460	167.11	4,053	88.6	17
YAG and CdS:Cu/ZnS	460	37	3,357	89	18
YAG and CdSe/CdS/ZnS	460	32	3,865	88	19
YAG and $K_2TiF_6:Mn^{4+}$	455	116	3,556	81	20
YAG and $Li_3Mg_2SbO_6:Mn^{4+}$	454	87	3,254	81	21
YAG and $Ba_{0.8}Sr_{0.2}Mg_3SiN_4:Eu^{2+}$	450	120	4,000	96	22
YAG and $Cs_2GeF_6:Mn^{4+}$	450	141.5	3,673	84.9	23
$Lu_3(Al/Ga)_5O_{12}:Ce^{3+}$ and $Ca_{1-x}Li_xAl_{1-x}Si_{1+x}N_3:Eu^{2+}$	450	101	3,036	95	24
$Lu_3(Al/Ga)_5O_{12}:Ce^{3+}$ YAG and $Sr[Li_2Al_2O_2N_2]:Eu^{2+}$	449	-	2,700	91	25
$RbNa_2K(Li_3SiO_4)_4:Eu^{2+}$, $(Sr,Ba)_2SiO_4:Eu^{2+}$ and $CaAlSiN_3:Eu^{2+}$	395	10.37	3,707	70.9	26
$CsNa_2K(Li_3SiO_4)_4:Eu^{2+}$, $(Sr,Ba)_2SiO_4:Eu^{2+}$ and $CaAlSiN_3:Eu^{2+}$	395	5.19	3,331	71.5	26
CdZnSeS/ZnS	390	222.7	6,029	95.1	27
Phosphor-in-glass [3]	385	27.19	2,984	84.2	28
Multi-color phosphor-in-glass	385	27.8	4,245	92.6	29
$(Ba,Sr,Ca)BP_2O_8:Eu^{2+}$ and $CaAlSiN_3:Eu^{2+}$	380	-	5,995	91	30
$Cs_{(1x)}Rb_xVO_3$	365	94.8	5,178	82	31
BAM, YAG	310	-	4,437	93.8	32
BAM and S2S	390	120	4,390	72	This study

[1] Tungsten filament, [2] Mercury-vapor and phosphors (λ_{exc} = 250 nm), [3] $CaAlSiN_3:Eu^{2+}$, $Ba_2MgSi_2O_7:Eu^{2+}$, and $(Sr,Ba)_3MgSi_2O_8:Eu^{2+}$.

Source: Own authorship.

The US Department of energy has brought up a multi-year program plan to overcome all the barriers that are currently found in SSL, Table 1.3.[6] In all those projections, the CRI value is expected to be greater than 85 and the CCT, lower than 4,500 K. It is important to decrease the CCT value of the commercial WLED because the human circadian system is exquisitely sensitive to blue-rich light, especially at night, leading to many diseases such as diabetes, insomnia, and depression.[33] Yet, although light may have undesirable consequences to human health depending on the wavelength and CCT, it may be useful in medical applications and indoor farms, in the last case, by increasing the biomass production rate of plants, opening up new and exciting frontiers in SSL engineering to fabricate high-brightness monochromatic LEDs for several applications, Table 1.4.[4]

Table 1.3 Target LE for different kind of WLED approach. λ_{em} represents the emission wavelength, FWHM is the full-width at half maximum of the emission band, RGB is the red, green and blue emission, RGBA is the red, green, blue and Amber emission, R_9 is the Munsell code for the red emission quantification, LE is the luminous efficacy, CM-LEDs are the color-mixed LEDs, and PC-LEDs are the phosphor-converted LEDs.

RGB CM-LED with CCT of 3,000 K and CRI of 85 (R9 > 0)				
Emissions	Blue LED	Green LED	Red LED	Representation
λ_{em} (nm)	464	546	612	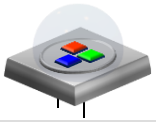
FWHM (nm)	20	20	20	
LE (lm/W)	Current		Target	
	133		191	
PC-LED with CCT of 3,000 K and CRI of 85 (R9 > 0)				
Emissions	Blue LED	Green phosphor	Red phosphor	Representation
λ_{em} (nm)	464	536	612	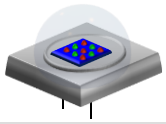
FWHM (nm)	20	100	100	
LE (lm/W)	Current		Target	
	123		189	
Hybrid-LED with CCT of 3,000 K and CRI of 85 (R9 > 0)				
Emissions	Blue LED	Green phosphor	Red LED	Representation
λ_{em} (nm)	459	539	612	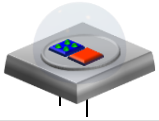
FWHM (nm)	20	100	20	
LE (lm/W)	Current		Target	
	165		231	
RGBA CM-LED with CCT of 3,000K and CRI of 85 (R9>0)				
Emissions	Blue LED	Green LED	Amber LED	Red LED	Representation
λ_{em} (nm)	460	539	590	615	
FWHM (nm)	20	20	20	20	
LE (lm/W)	Current		Target		
	85		153		

Source: Own authorship.

Table 1.4 Monochromatic LEDs for human phototherapy and plant and food technology.

LED emission spectral range	Application for human healthy	Application for plant and food technology
Red (630 nm)	Rhinitis treatment, wound healing and anti-inflammatory[34]	Algae growth, microalgae cultivation, plant tissue culture[34]
Green (550 nm)	Correct hyperpigmentation, eliminate skin spots[35]	Algae growth, bacteria and microalgae cultivation[34]
Blue (480 nm)	Seasonal Affective Disorder (SAD), non-seasonal depression and bipolar disorder therapies[9]	Algae growth, astaxanthin production[34]
UV (250 nm)	Disinfection, water treatment[34]	Disinfection, water treatment [34]

Source: Own authorship.

The main commercially-available monochromatic LEDs are based on AlInGaN or AlGaInP (Indium aluminum gallium nitrite or Aluminum gallium indium phosphide) semiconductor and their bandgap may be tuned from 0.7 eV to 3.4 eV by changing the composition, within the 365 – 1,900 nm spectral range.[36] Nonetheless, the main challenge on the fabrication of monochromatic LEDs lies on the previously mentioned “green gap”, i.e., the absence of high-efficient semiconductors in the green spectral region. This issue

arises from the abrupt decrease of the external quantum efficiency (EQE) of the InGaN-based LEDs in the green-yellowish spectral range. On the other hand, the EQE of the AlGaInP-based LEDs increases only from 600 nm, as represented in Figure 1.3.[36]

Figure 1.3 External quantum efficiency of conventional monochromatic LEDs emitting in the visible spectral region.

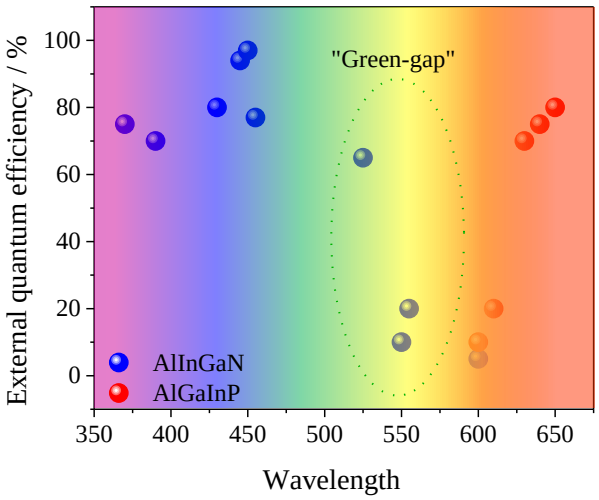

Source: Adapted from Seong *et al.*[37]

To address the "green gap" drawback, a feasible alternative is combining a near-UV-emitting LED chip (near-UV LED) with near-UV-to-green downshifting converter phosphors thanks to the huge improvement of the WPE of near-UV LEDs achieved in the last few years.[38] Therefore, the main challenge on the fabrication of high-efficient white or monochromatic LEDs lies on the improvement of the phosphor properties as the emission quantum yield and the thermal and structural stabilities.

In this study, we have chosen silicate-based phosphors, well-known as coatings of PC-LEDs. The state-of-the-art of Ba_2SiO_4 and Sr_2SiO_4 based-phosphors comparing the emission quantum yield and the annealing temperature as figures of merits is shown in Table 1.5.

Table 1.5 Figure of merit of the emission quantum yield (q) of M_2SiO_4:RE (M = Sr or Ba and RE = Eu^{2+}, Eu^{3+} or Tb^{3+}) phosphors. The excitation wavelength (λ_{exc}), emission wavelength (λ_{em}) and the calcination temperature (T. calc.) to get the phase are also provided.

Sample	T. calc. / ºC	λ_{exc}/ nm	λ_{em}/ nm	q / %	[ref]
$Ba_2SiO_4:Eu^{2+}$	1,200	450	508	0.53	39
$Sr_2SiO_4:Eu^{2+}$	1,200	400	550	0.60	39
$Ba_2SiO_4:Eu^{3+}$	1,300	250	612	-	43
$Ba_2SiO_4:Tb^{3+}$	1,450	250	545	-	40
$Ba_2SiO_4:Eu^{3+}$, Tb^{3+}	-	-	-	-	-

Source: Own authorship.

In this study, attention was placed on the improvement of the synthesis of silicate-based phosphors, since, although there are several methods for the phosphor obtention,[41,42,43] some points as high calcination temperature (1,200 ºC-1,500 ºC) and low emission quantum yield (50 %) still need to be addressed.

To contextualize, the Ba_2SiO_4 matrix is a current subject of research in the LLuMeS research group. The study of this host for rare earth ions has started at about in 1995 [44] with Professor Ana Maria Pires under supervision of Professor Marian Rosaly Davolos. In this study, it was investigated the barium silicate matrix synthesis by the solid-state route and its use as host for Eu^{2+} and/or Eu^{3+} as precursor for $BaZnSiO_4:Eu^{3+},Mn^{2+}$ phosphor for application in fluorescent lamp.[45]

In 2010, Master Diego Ariça Ceccato started, in LLuMeS laboratory, the investigation of the Ba_2SiO_4 synthesis by the sol-gel route, and its use as an electrochemical sensor.[46] Finally, taking advantage of the sol-gel synthesis, we started in 2013 a scientific initiation scholarship to optimize the Eu^{3+} concentration in the Ba_2SiO_4 host. Then, in 2015, during the Ph.D., we have started to develop all the study showed in this thesis.

1.2 Motivation, challenges and justifications

We got involved in this study motived by three main points: (i) to apply deep-UV-to-visible downshifting converter phosphors as coatings of deep-UV-emitting LEDs, fabricating multifunctional UV and visible-emitting LED prototypes to be used in indoor farms, (ii) to work around the “green gap” issue by coating near-UV-emitting LEDs with $Ba_2SiO_4:Eu^{2+}$ green-emitting phosphors, making green-emitting LED prototypes and (iii) to improve the color qualities of WLEDs by combining near-UV-to-visible downshifting converter phosphors and commercial near-UV-emitting LED chips.

The reason behind point (i) lies on the potential application of a multifunctional UV and visible-emitting LED in indoor farms because of the UV radiation may be applied as an antibacterial agent, and the visible light is helpful to enhance the photosynthesis rate, by controlling the plant Circadian rhythm, as previously highlighted in Table 1.4.

Already about point (ii), the use of near-UV-emitting LEDs coated by green-emitting phosphors seems to be an alluring approach to overcome the “green gap” drawback.

Considering point (iii), there are many challenges to be overcome concerning the fabrication of high-efficient and stable WLEDs with desirable CCT and CRI values such as (a) the fabrication of thermally-stable phosphors with high emission quantum yield, (b) to elect an ideal phosphor mix to fill all the visible spectrum in order to get desirable color qualities, (c) to get photostable LED prototypes with no changes in the color emission over the time of use and (d) how to process the phosphor particles as coatings.

To cope with point (i), we chose to synthesize red-emitting phosphors based on $Ba_2SiO_4:Eu^{3+}$ and blue or green-emitting phosphors based on $Ba_2SiO_4:Tb^{3+}$, all processed as polymeric films. Already to fill points (ii) and (iii), we chose the $Ba_2SiO_4:Eu^{2+}$ and $Sr_2SiO_4:Eu^{2+}$ phosphors, respectively, dispersed in polymeric films.

The justifications on their selection lie on the thermal stability (1,000 ºC), relatively low phonon frequency of the matrices (800 cm^{-1}), transparency to UV radiation, desirable emission quantum yield, and the possibility of hosting divalent and trivalent dopant cations. The role of the phosphor processing as films lies on the decrease of the light scattering, and the improvement of the heat dissipation, to which are drawbacks currently found in the traditional protocol for the phosphor processing as coatings of LED chips (dispersion in silicone, epoxy resin or polyurethane).

1.3 Goals

The goal of this study is to fabricate light-emitting diodes by coating UV-emitting LED chips with UV-to-visible downshifting converter phosphors dispersed in polymeric matrices, in order to come up with prototypes featuring potential to be applied in lighting, devices, agriculture or phototherapy through the control of the Circadian rhythm of plants and humans, Figure 1.4.

The specific goals are:

1. To synthesize deep-UV-to-visible downshifting converter phosphors based on Eu^{3+} and/or Tb^{3+} doped Ba_2SiO_4 phosphor;
2. To use Eu^{3+} as spectroscopic probe aiming to understand the impacts of the doping on the Ba_2SiO_4 network;
3. To understand the energy transfer process between $Tb^{3+} – Tb^{3+}$ and $Eu^{3+} – Tb^{3+}$ in the Ba_2SiO_4 matrix;
4. To elect a suitable polymeric matrix to disperse the phosphors in order to make films with controlled thickness;

5. To use the $Ba_2SiO_4:Eu^{3+},Tb^{3+}$ phosphor as coatings of deep-UV-emitting LEDs;

6. To synthesize a green-emitting phosphor based on $Ba_2SiO_4:Eu^{2+}$ and use it as coating of near-UV emitting chips in order to fabricate green-emitting LED prototypes;

7. To synthesize a yellow-emitting phosphor based on $Sr_2SiO_4:Eu^{2+}$ and use it as coating of near-UV emitting chips combined to a blue-emitting phosphor ($BAM:Eu^{2+}$), aiming to fabricate a WLEDs featuring tunable CCT.

Figure 1.4. Goals of the thesis.

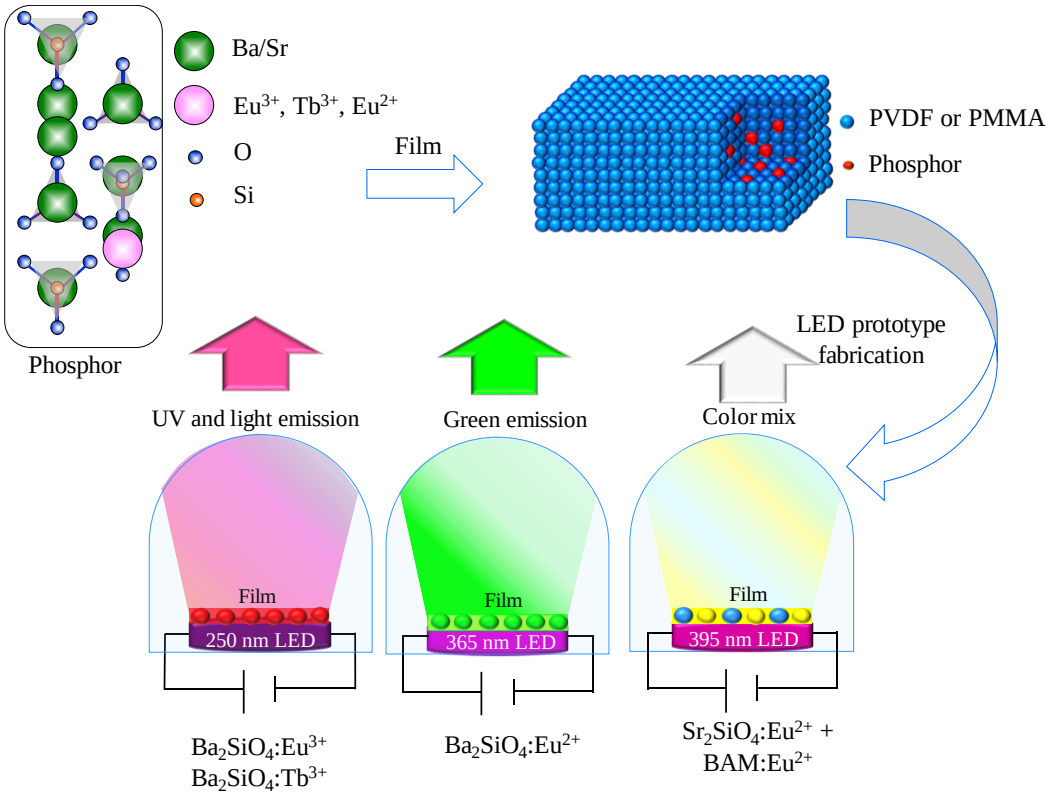

Source: Own authorship.

1.4 Thesis organization

Chapter 1 – Introduction: Discussion on the state-of-the-art of LEDs and silicate-based phosphors.

Chapter 2 - Background: Presentation of the main concepts used to discuss the results.

Chapter 3 – Tunable blue-green emission and energy transfer properties in $Ba_2SiO_4:Tb^{3+}$: Discussion on the synthesis of green/blue-emitting phosphors, impacts of the Tb^{3+}-doping on the Ba_2SiO_4 network, energy transfer properties and quantum efficiency of Tb^{3+}. This chapter was written based on a paper published in the Journal of Luminescence.[47]

Chapter 4 – Sol-gel synthesis of Eu^{3+}-doped Ba_2SiO_4: Synthesis of red-emitting phosphors, optimization of the synthesis and impacts of the doping on the defect-related structure of the Ba_2SiO_4 lattice. Part of this chapter was written based on a paper published in the RSC Advances.[48]

Chapter 5 – Energy transfer between Tb^{3+} and Eu^{3+} in barium orthosilicate phosphors. Discussion on the tunable red-blue light emission in $Ba_2SiO_4:Eu^{3+},Tb^{3+}$, energy transfer properties and use of Tb^{3+} as a sensitizer to Eu^{3+}. This chapter was written based on a paper published in the Journal of Luminescence.[49]

Chapter 6 – Red-light-emitting coatings for LEDs applied to plant circadian rhythm control: Fabrication of polymeric films containing $Ba_2SiO_4:Eu^{3+}$ and evaluation of these films as coatings of deep-UV-emitting LEDs. Part of this chapter was written based on a paper published in the Materials Chemistry and Physics.[50]

Chapter 7 - Green-emitting LEDs based on $Ba_2SiO_4:Eu^{2+}$ and near-UV-emitting LEDs: Synthesis of the $Ba_2SiO_4:Eu^{2+}$ phosphor in the powder form or dispersed in PMMA and fabrication of green-emitting LEDs.

Chapter 8 - White-emitting LEDs based on Eu^{2+}-doped silicate: Synthesis of the $Sr_2SiO_4:Eu^{2+}$ phosphor in the powder form or dispersed in PMMA and fabrication of white-emitting LEDs.

Chapter 9 – Final remarks: Presentation of the final remarks and some proposals for future studies in the research group.

1.5 References

[1] FRIEDEL, R. D.; ISRAEL, P.; FINN, B. S. Edison's electric light, Bibliography, 1987, Rutgers University Press.

[2] CHO, J. et al. White light-emitting diodes: History, progress, and future, Laser & Photonics Reviews, 2017, v. 11, n. 2, p. 1600147-17.

[3] JACOBY, M. Tuning phosphors for better white light Advances in the inorganic powders boost the efficiency and appeal of LED bulbs, Chemical and Engineering News, 2018, v. 96, n. 46, p. 28-33.

[4] PATTISON, P. M; HANSEN, M.; TSAO, J. Y. LED lighting efficacy: Status and directions, Comptes Rendus Physique, 2018, v. 19, n. 3, p. 134-145.

[5] MITCH JACOBY, Tuning phosphors for better white light, C&EN, 2018, v. 96, n. 46, p. 28-33.

[6] BARDSLEY, N. et al. Solid-State Lighting Research and Development Multi-YearProgram Plan, Building Technologies Office, Office of Energy Efficiency and Renewable Energy, U.S. Department of Energy, 2014 (DOE/EE-1089).

[7] CHEN, L. et al. Light Converting Inorganic Phosphors for White Light-Emitting Diodes, Materials, 2010, v. 3, n. 3, p. 2172-2195.

[8] BAI, X. et al. Efficient and tuneable photoluminescent boehmite hybrid nanoplates lacking metal activator centres for single-phase white LEDs, Nature Communications, 2014, v. 5, n. 0, p. 5702-8.

[9] LEGATES, T. A.; FERNANDEZ, D. C.; HATTAR, S. Light as a central modulator of circadian rhythms, sleep and affect, Nature Reviews, 2014, v. 15, n. 7, p. 443–454.

[10] OH, J. H.; YANG, S.J.; DO, Y. R. Healthy, natural, efficient and tunable lighting:four-package white LEDs for optimizing the circadian effect, color quality and vision performance, Light: Science & Applications, 2014, v. 3, n. 0, p. 141-9.

[11] ZHAO, M. et al. Next-Generation Narrow-Band Green-Emitting $RbLi(Li_3SiO_4)_2:Eu^{2+}$ Phosphor for Backlight Display Application, Advanced Materials, 2018, v. 30, n. 38, p. 1802489-7.

[12] PATTISON, P. M. et al. LEDs for photons, physiology and food, Nature, 2018, v. 543, n. 0, p. 493 – 500.

[13] HONG, F. et al. Room-temperature synthesis, optimized photoluminescence and warm-white LED application of a highly efficient non-rare-earth red Phosphor, Journal of Alloys and Compounds, 2019, v. 775, n. 0, p. 1365-1375.

[14] LV, L. et al. The formation mechanism, improved photoluminescence and LED applications of red phosphor $K_2SiF_6:Mn^{4+}$, Journal of Materials Chemistry C, 2014, v. 2, n. 20, p. 3879–3884.

[15] ZHENG, F. et.al, Reliability of fluoride phosphor $K_2XF_6:Mn^{4+}$ ($K_2SiF_6:Mn^{4+}$, $K_2(Si,Ge)F_6:Mn^{4+}$, $K_2TiF_6:Mn^{4+}$) for LED application, Journal of Materials Science: Materials in Electronics, 2018, v. 29, n. 24, p. 21061–21071.

[16] JIANG, C, et al. Mn^{4+}-Doped Heterodialkaline Fluorogermanate Red Phosphor with High Quantum Yield and Spectral Luminous Efficacy for Warm-White-Light-Emitting Device Application, Inorganic Chemistry 2018, v. 57, n. 23, p. 14705−14714.

[17] DENG, T. et al. Implementation of high color quality, high luminous warm WLEDusing efficient and thermally stable $Rb_3AlF_6:Mn^{4+}$ as red color converter, Journal of Alloys and Compounds, 2019, v. 795, n. 0, p. 453-461.

[18] WANG, X. et al. Doped Quantum Dots for White-Light-Emitting Diodes Without Reabsorption of Multiphase Phosphors, Advanced Materials, 2012, v. 24, n.20, p. 2742–2747.

[19] WANG, X. LI, W. SUN, K. STABLE efficient CdSe/CdS/ZnS core/multi-shell nanophosphors fabricated through a phosphine-free route for white light-emitting-diodes with high color rendering properties, Journal of Materials Chemistry, 2011, v. 21, n. 24, p. 8558-8565.

[20] ZHU, H. et al. Highly efficient non-rare-earth red emitting phosphor for warm white light-emitting diodes, Nature communications, 2014, v. 5, n. 0, p. 4312-10.

[21] WANG, S. et al. Mn^{4+}-activated $Li_3Mg_2SbO_6$ as an ultrabright fluoride-free red-emitting phosphor for warm white light-emitting diodes, RSC Advances, 2019, v. 9, n. 6, p. 3429- 3435.

[22] OSBORNE, R. A. et al. $Ba_{(1-x)}Sr_xMg_3SiN_4$:Eu narrow band red phosphor, Optical Materials, 2018, v. 84, n. 0, p. 130–136.

[23] WANG, Z. et al. Highly efficient red phosphor $Cs_2GeF_6:Mn^{4+}$ for warm white light-emitting diodes, RSC Advances, 2015, v. 5, n. 100, p. 82409-82414.

[24] WANG, L. et al. $Ca_{1-x}Li_xAl_{1-x}Si_{1+x}N_3:Eu^{2+}$ solid solutions as broadband, color-tunable and thermally robust red phosphors for superior color rendition white light-emitting diodes, Light: Science & Applications, 2016, v. 5, n. 0, p. 16155.

[25] HOERDER, G. J. et al. $Sr[Li_2Al_2O_2N_2]:Eu^{2+}$—A high performance red phosphor to brighten the future, Nature Communications, 2019, v. 10, n. 0, p. 1824-9.

[26] ZHAO, M. et al. Discovery of New Narrow-Band Phosphors with the UCr4C4-Related Type Structure by Alkali Cation Effect, Advanced Optical Materials, 2018, v. 1801631, n. 6, p. 1-9.

[27] LE, T. et al. Highly Luminescent Quantum Dots in Remote-Type Liquid-Phase Color Converters for White Light-Emitting Diodes, Advanced Materials Technology, 2018, v. 3, n. 3, p. 1800235-9.

[28] PENG, Y. et al. Luminous efficacy enhancement of ultraviolet-excited white light-emitting diodes through multilayered phosphor-in-glass, Applied Optics, 2016, v. 55, n. 18, p. 4933- 4938.

[29] JIANG, P. Thermally stable multi-color phosphor-in-glass bonded on flip-chip UV-LEDs for chromaticity tunable WLEDs, Applied Optics, 2017, v. 56, n. 28, p. 7921- 7926.

[30] SU, S. et al. Near UV-pumped bluish-white emitting K(Ba,Sr,Ca)BP_2O_8:Eu^{2+} phosphors, Journal of Alloys and Compounds Volume. 2013, v. 575, n. 0, p. 309-313.

[31] PAVITRA, E. et al. Evolution of highly efficient rare-earth free $Cs_{(1x)}Rb_xVO_3$ phosphors as a single emitting component for NUV-based white LEDs, Journal of Materials Chemistry C, 2018, v. 6, n. 46, p. 12746- 12757.

[32] Li, H. et al. Synthesis and Luminescence Properties of Bi^{3+}-Activated K_2MgGeO_4: A Promising High-Brightness Orange-Emitting Phosphor for WLEDs Conversion, Inorganic Chemistry, 2018, v. 57, n. 19, p. 12303−12311

[33] FIGUEIRO, M. G. An Overview of the Effects of Light on Human Circadian Rhythms: Implications for New Light Sources and Lighting Systems Design, Journal of Light & Visual Environment, 2013, v. 37, n. 2, p. 51-61.

[34] YEH, N. et al. Applications of light-emitting diodes in researches conducted in aquatic environment, Renewable and Sustainable Energy Reviews, 2014, v. 32, n.0, p. 611–618.

[35] KLEIN, R. M. Effects of green light on biological systems, Biological reviews of the Cambridge Philosophical Society, 1992, v. 67, n. 2, p.199-284.

[36] JEONG, H. et al. Indium gallium nitride-based ultraviolet, blue, and green light emitting diodes functionalized with shallow periodic hole patterns, Scientific Reports, 2017, v. 7, n. 0, p. 45726-9.

[37] SEONG, T. et al. III-Nitride Based Light Emitting Diodes and Applications, Topics in Applied Physics, 2013, springer.

[38] MATAFONOVA, G. BATOEV, V. Recent advances in application of UV light-emitting diodes for degrading organic pollutants in water through advanced oxidation processes: A review, Water Research, 2018, v. 132, n. 1, p. 177-189.

[39] SATO, Y. et al. Large redshifts in emission and excitation from Eu^{2+} activated Sr_2SiO_4 and Ba_2SiO_4 phosphors induced by controlling Eu^{2+} occupancy on the basis on crystal-site engineering, Optics and Photonics Journal, 2015, v. 5, n. 11, p. 326-333.

[40] DA-WEI, H. et al. VUV Luminescent Properties of M_2SiO_4:Re (M =Mg, Ca, Ba) (Re= Ce^{3+}, Tb^{3+}), Chinese Journal of Luminescence, 2007. v. 28, n.1, p. 53-57.

[41] AWATE, V. et al. Synthesis, characterization and luminescence studies of rare earth activated Sr_2SiO_4 phosphor: a review, Journal of Materials Science: Materials in Electronics, 2018, v. 29, n.6, p. 4391–4401.

[42] SZCZODROWSKI, K. et al. The role of compensation defects in Eu^{3+} stabilization under reductive atmosphere in Sr_2SiO_4 matrix, Journal of Alloys and Compounds, 2018, v. 748, n.5, p. 44-50.

[43] WANG, Z. et al. Luminescent properties of Ba_2SiO_4:Eu^{3+} for white light emitting diodes, Physica B, 2013, v. 411, n.15, p. 110–113.

[44] PIRES, A. M.; DAVOLOS, M. R.; MALTA, O.L. Eu^{3+}-O^{2-}associates luminescence in Ba_2SiO_4, Journal of Luminescence, 1997, v. 72-74, n. 0, p. 244-246.

[45] PIRES, A. M.; DAVOLOS, M. R. Luminescence of Europium(III) and Manganese(II) in Barium and Zinc Orthosilicate, Chemistry of Materials, 2001, v. 13, n. 1, p. 21-27.

[46] RAYMUNDO-PEREIRA, et al. Study on the structural and electrocatalytic properties of Ba^{2+}- and Eu^{3+}-doped silica xerogels as sensory platforms. RSC Advances, 2016, v. 6, n. 106, p. 104529-104536.

[47] BISPO-JR, A.G. et al. Tunable blue-green emission and energy transfer properties in Ba_2SiO_4:Tb^{3+} obtained from sol-gel method, Journal of luminescence, 2019, v. 214, n. 0, p. 116604-8.

[48] BISPO-JR, A. G. et al. Red phosphor based on Eu^{3+}-isoelectronically doped Ba_2SiO_4 obtained via sol–gel route for solid state lightning, RSC Advances, 2017, v. 7, n. 85, p. 53752–53762.

[49] BISPO-JR, A. G. et al. Energy transfer between terbium and europium ions in barium orthosilicate phosphors obtained from sol-gel route, Journal of Luminescence, 2018, v. 199, n. 0, p. 372–378.

[50] BISPO-JR, A. G. et al. Red-light-emitting polymer composite based on PVDF membranes and Europium phosphor using Buriti Oil as plasticizer, Materials Chemistry and Physics, 2018, V 217, n. 0, p. 160-167.

that the WLED prototypes appeal as attractive alternatives to be applied in lighting, traffic signs, displays as well as phototherapy.

8.6 References

[1] PATTISON, P. M. et a. LEDs for photons, physiology and food, Nature, 2018, v. 563. n. 0, p. 493 – 500.

[2] OH, J. H.; YANG, S. J.; DO, Y. R. Healthy, natural, efficient and tunable lighting: four-package white LEDs for optimizing the circadian effect, color quality and vision performance, Light: Science & Applications, 2014, v. 3, n. 0, p. e141.

[3] YOO, H. C. et al. Circadian-tunable Perovskite Quantum Dot-based Down-Converted Multi-Package White LED with a Color Fidelity Index over 90, Nature, 2017, v. 7, n. 0, p. 2808-11.

[4] KIM, D. et al. Wide range yellow emission $Sr_8MgLa(PO_4)_7$: Eu^{2+}, Mn^{2+},Tb^{3+} phosphors for near ultraviolet white LEDs, Materials Research Bulletin, 2018, v. 107, n. 0, p. 280–285.

[5] YU, L. et al. Cation vacancy repair for the enhancement of orange-yellow luminescence in $Sr_9Mg_{1.5\_x}K_x(PO_4)_7$:$Eu^{2+}$ phosphors, Journal of Materials Chemistry C, 2018, v. 6, n. 40, p. 10723-10729.

[6] ARTINI, C. et al. Rare-Earth-Doped Ceria Systems and Their Performance as Solid Electrolytes: A Puzzling Tangle of Structural Issues at the Average and Local Scale, Inorganic Chemistry, 2018, v. 57, n. 21, p. 13840−13846.

[7] RAYMUNDO-PEREIRA, P. A. et. Al. Study on the structural and electrocatalytic properties of Ba^{2+}- and Eu^{3+}-doped silica xerogels as sensory platforms, RSC Advances, 2016, v. 6, n. 106, p. 104529-104536.

[8] HAN, J. K. et al. Structure dependent luminescence characterization of green–yellow emitting Sr_2SiO_4:Eu^{2+} phosphors for near UV LEDs, Journal of Luminescence, 2012, v. 132, n. 1, p. 106–109.

[9] CATTI, M. GAZZONI, G. The β -α' phase transition of Sr_2SiO_4. II. X-ray and optical study, and ferroelasticity of the β form, Acta Crystallography B, 1983, v. 39, n. 39, p. 679-684.

[10] PARK, J. H.; AHN, W.; KIM Y. J. Phase formation and luminescence of Sr_2SiO_4:Eu^{2+} nanopowders prepared by a hybrid process, Ceramics International, 2015, v. 41, n. 1, p. S734–S739.

[11] LEE, J. S.; Kim, Y. J. Synthesis and Luminescent characterization of Sr_2SiO_4:Eu^{2+} nanopowders, J. Nanoscience and Nanotechnology, 2012, v. 12, n. 11, p. 8630–8634.

[12] XIE, R. et al. A Simple, Efficient Synthetic Route to $Sr_2Si_5N_8$:Eu^{2+}-Based Red Phosphors for White Light-Emitting Diodes, Chemistry of Materials, 2006, v. 18, n. 23, p. 5578-5583.

[13] HAN, J. K. et al. Structure dependent luminescence characterization of green–yellow emitting Sr_2SiO_4:Eu^{2+} phosphors for near UV LEDs, Journal of Luminescence, 2012, v. 132, n. 1, p. 106–109.

[14] Nasir, S. S. B. et Al. Luminescence properties of Li_2SrSiO_4:Eu^{2+} silicate yellow phosphors with high thermal stability for high-power efficiency white LED application, Journal of Luminescence, 2019, v. 207, n. 0, p. 22–28.

[15] LU, Z. et al. Hydrothermal synthesis, morphology and photoluminescence of hexagonal $SrSiO_3$:Eu^{2+} micro-octahedrons and prism-like hollow microstructures, Materials Chemistry and Physics, 2012, v. 132, n. 2-3, p. 800– 807.

[16] BIRKEL, A. et al. Eu^{2+}-doped M_2SiO_4 (M = Ca, Ba) phosphors prepared by a rapid microwave-assisted sol-gel method: Phase formation and optical properties, Solid State Sciences, 2013, v. 19, n. 0, p. 51-57.

[17] LIZZO, S. et al. The luminescence of Eu^{2+} in magnesium fluoride crystals, Journal of Luminescence, 1995, v. 65, n. 6, p. 303–311.

[18] CHASE, L. L. et al. Microwave-optical double resonance of the metastable $4f^65d$ level of Eu^{2+} in the fluorite lattices, Physics Review B, 1970, v. 2, n. 7, p. 2308–2318.

[19] ZELER, J. et al. Fine structure in high resolution $4f^7$–$4f^65d$ excitation and emission spectra of X-ray induced Eu^{2+} centers in $LuPO_4$:Eu sintered ceramics, Journal of Luminescence, 2019, v. 207, n. 0, p. 435–442.

[20] BINNEMANS, K. Interpretation of Europium(III) spectra, Coordination Chemistry Reviews, 2015, v. 295, n. 0, p. 1–45.

[21] HAN, N. S. et al. Defect states of ZnO nanoparticles: Discrimination by time-resolved photoluminescence spectroscopy, Journal of applied physics, 2010, v. 107, n. 8, p. 084306-7.

[22] SETLUR, A. A.; SHIANG, J. J.; HAPPEK U. Eu^{2+} - Mn^{2+} phosphor saturation in 5 mm light emitting diode lamps, Applied physics letters, 2008, v. 92, n. 8, p. 081104-3.

[23] GEORGE, N. C.; DENAULT, K. A.; SESHADRI, R. Phosphors for solid-state white lighting. Annual Review of Materials Research, 2013, v. 43, n. 0, p. 481–501.

[24] PARK, J. K. et al. White light-emitting diodes of GaN-based Sr_2SiO_4:Eu and the luminescent properties, Applied Physics Letters, 2003, v. 82, n. ,8 p. 683-685.

[25] LE, T. et al. Highly Luminescent Quantum Dots in Remote-Type Liquid-Phase Color Converters for White Light-Emitting Diodes, Advanced Materials Technology, 2018, v. 3, n. 11, p. 1800235.

[26] CHO, I. H. et al. On the stability and reliability of $Sr_{1-x}Ba_xSi_2O_2N_2:Eu^{2+}$ phosphors for white LED applications, Optical Materials Express, 2012, v. 2, n. 9, p. 1294-1305.

[27] RAHMAN, F. et al. Short- and Long-Term Reliability Studies of Broadband Phosphor-Converted Red, Green, and White Light-Emitting Diodes, IEEE transactions on device and materials reliability, 2016, v. 16, n. 1, p. 1-8.

[28] JIANG, P. et al. Thermally stable multi-color phosphor-in-glass bonded on flip-chip UV-LEDs for chromaticitytunable WLEDs, Applied Optics, 2017, v. 56, n. 28, p. 7921-7926.

[29] BAI, X. et al. Efficient and tuneable photoluminescent boehmite hybrid nanoplates lacking metal activator centres for single-phase white LEDs, Nature communications, 2014, v. 5, n. 5702, p. 1-8.

CHAPTER 9 – FINAL REMARKS

9.1 Conclusions

In this study, UV-to-blue ($Ba_2SiO_4:Tb^{3+}$), green ($Ba_2SiO_4:Tb^{3+}$ and $Ba_2SiO_4:Eu^{2+}$), yellow ($Sr_2SiO_4:Eu^{2+}$) and red ($Ba_2SiO_4:Eu^{3+}$) downshifting converter phosphors were synthesized by the sol-gel route and dispersed in polymeric matrices (PVDF or PMMA), making films that were used as coatings of UV LEDs, fabricating green, yellow, and white-emitting LED prototypes.

All phosphors were synthesized in softer calcination conditions (1,100 ºC-1,200 ºC) than the tradition solid-state route (> 1,200 ºC) and their dispersion in the PMMA polymer seems to be an alluring alternative to enhance the luminescent features of the films since PMMA undo superficial defects in the phosphor network, enhancing the emission quantum yield. Yet, although the phosphor dispersion in PVDF may enhance the phosphor emission, the low amount dispersed in the polymer (10 wt.%) is a remarkable drawback compared to PMMA.

$Ba_2SiO_4:Tb^{3+}$ was synthesized as monophasic phase and as the Tb^{3+} amount increases from 0.1 % to 5 %, the overall emitted color dislocates from the blue toward the green spectral region due to a cross-relaxation energy transfer by a dipole-dipole mechanism. We also introduced a simple approach to calculate the $^5D_3$ state quantum efficiency from the emission spectrum, and these values decrease as the Tb^{3+} amount increases in the lattice.

Already the $Ba_2SiO_4:Eu^{3+}$ phosphor displays the usual Eu^{3+} emission in the red spectral region. Eu^{3+} is inserted in 8 non-equivalent local sites, 2 from the replacement of Ba^{2+} in the Ba_2SiO_4 lattice, 1 in the $BaSiO_3$ spurious phase (trace), 2 in Eu^{3+}-O^{2-} associates and 3 defect-related sites. It is worth pointing out that Tb^{3+} may act as a sensitizer for the Eu^{3+} luminescence in the case that the Tb^{3+} content is much lower than the Eu^{3+} one.

Considering the $Ba_2SiO_4:Eu^{3+}$ features for applications in multifunctional LEDs for indoor farm application, its emission quantum yield (11 %) is among the best considering silicate-based phosphors, but it is lower than the classical red-emitting phosphors. Finally, the PMMA/$Ba_2SiO_4:Eu^{3+}$ films were tentatively applied as coatings of deep-UV emitting LEDs (250 nm), but the low external quantum efficiency of the UV LED limits the real use of the prototype.

The $Ba_2SiO_4:Eu^{2+}$ green-emitting phosphor features a thermally stable broad emission band in the green spectral region and its emission quantum yield increases from

0.27±0.03 up to 0.50±0.05 after the dispersion in PMMA. The PMMA/$Ba_2SiO_4:Eu^{2+}$ films were used as coatings of near-UV emitting LEDs (365 nm), making green-emitting LED prototypes with luminous efficacy and reliability among the best already reported, thus, being an alternative to work around the "green gap" and be used as traffic light, backlight of displays and mainly in phototherapy.

$Sr_2SiO_4:Eu^{2+}$ yellow emitting phosphor was combined to the commercial BAM blue-emitting phosphors, making tunable white-light-emitting films, to which were used to coat near-UV-emitting LEDs (395 nm). By changing the phosphor mix in the WLED prototypes, the CCT values dislocate from 5,412 K (ideal for daylight application) toward 3,346 K (ideal for nigh light application), being that all the prototypes feature luminous efficacy and reliability among the best already reported. Therefore, these prototypes match the required characteristics to be used in lighting, backlight of displays and in phototherapy, by regulating the human circadian rhythm, following the sunlight changes over the day.

Finally, the main contributions of this thesis to the solid-state lighting field are summarized by the following three points. (1) Although the "green-gap" is still a challenge considering green-emitting LEDs fabricated by semiconductors, this study evidences that it is possible to fabricate efficient and photostable green-emitting LEDs by coating UV LEDs with green-emitting phosphors, and these prototypes appeal as an alternative to replace the commercial LEDs, to which features high power consumption and low luminous efficacy. (2) The phosphor processing as coatings of LEDs is an important step considering the optimization of the luminous efficacy, and homogenous films based in PMMA containing the phosphor particles now are an alluring protocol for that. (3) The use of PC-WLEDs may achieve the luminous efficacy displayed by the YAG-based WLED.

9.2 Perspectives for futures investigations

After the end of this study, there are some points that may be further investigated in future studies in the LLuMes research group, and we highlight some of them:

1) To investigate other approaches for the charge-balancing in the $Ba_2SiO_4:Eu^{3+}$ and $Ba_2SiO_4:Tb^{3+}$ phosphors, for instance, by using alkaline ions as Li^+, Na^+ and K^+, or Al^{3+} to replace Si^{4+}.